Letters

A High-Efficiency Asymmetrical Half-Bridge Converter With Integrated Boost Converter in Secondary Rectifier

Jung-Kyu Han, *Student Member, IEEE*, Jong-Woo Kim, *Member, IEEE*, and Gun-Woo Moon, *Member, IEEE*

***Abstract*—A conventional asymmetrical half-bridge (AHB) converter is one of the most promising topologies in low-to-medium power applications because of zero-voltage switching of all switches and small number of components. However, when the converter is designed taking a hold-up time into consideration, it has a large DC offset current in a transformer and a small transformer turns-ratio. To solve these problems, a new AHB converter with an integrated boost converter is proposed in this letter. Because the proposed converter compensates for the hold-up time using the integrated boost converter without additional loss in the nominal state, it can achieve the optimized efficiency regardless of the hold-up time. The effectiveness and feasibility are verified with a 250–400-V input and 45 V/3.3 A output prototype.**

***Index Terms*—Asymmetrical half-bridge (AHB) converter, DC/DC converter, high efficiency, hold-up time.**

I. Introduction

In MANY applications such as TVs and PCs, power supplies should maintain an output voltage for a moment after an input AC line is lost. Generally, the output voltage should remain for tens of milliseconds after the AC loss, and this duration is called the hold-up time [1]–[4]. Since the DC/DC converter operates using the energy stored in the link capacitor located between the PFC converter and the DC/DC converter, the voltage of the link capacitor decreases during the hold-up time resulting in a decrease of the input voltage of the DC/DC converter. As a result, the DC/DC converter should be designed considering a wide input voltage range due to the hold-up time.

Among the various DC/DC converter topologies, the asymmetrical half-bridge (AHB) converter is one of the most promising topologies in low-to-medium power applications because of the zero-voltage switching (ZVS) of all switches, a small number of components, and a clamped voltage stress of primary switches [5]–[13]. However, the AHB converter has several problems when it is designed with a wide input voltage range. Since the AHB converter has the maximum voltage gain with 0.5 duty-ratio, it has increasing duty-ratio during the hold-up time, which results in small duty-ratio in the nominal state. As a result, the AHB converter has a small turns-ratio and large DC offset current in the transformer [5]–[9].

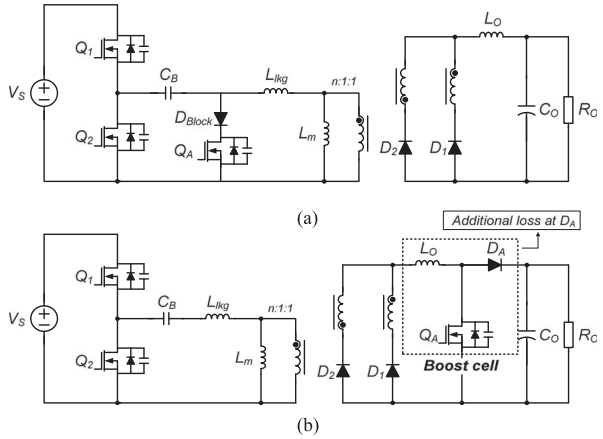

Fig. 1. Conventional AHB converters. (a) DCS HB converter and (b) boost-cascaded AHB converter.

Several studies have been done to overcome the drawbacks of the conventional AHB converter in wide input voltage range [10]–[13]. Among them, the duty-cycle-shifted half-bridge (DCS HB) converter shown in Fig. 1(a) eliminates the DC offset current by controlling the half-bridge switches symmetrically [12]. And ZVS operation of all switches is ensured with duty-cycle-shifted gate signal of switch Q_2 and freewheeling switch Q_A. However, the problem caused by the small transformer turns-ratio still remains in the DCS HB converter resulting in large primary RMS current and large voltage stress on the rectifier diodes because it also has the maximum gain with 0.5 duty-ratio. Furthermore, the freewheeling current flowing through the additional components causes additional conduction losses.

A boost-cascaded AHB converter shown in Fig. 1(b) solves the problem of the wide input voltage range [13]. It constitutes a cascaded boost converter by adding a switch and a diode to the secondary side while sharing the output inductor. In the nominal state, the additional switch Q_A is turned off, and the boost-cascaded AHB converter operates the same

Manuscript received December 29, 2016; revised January 28, 2017; accepted February 14, 2017. Date of publication February 24, 2017; date of current version June 23, 2017. This work was supported by the National Research Foundation of Korea (NRF) grant funded by the Korea government (MSIP) (2016R1A2B2010328).

J.-K. Han and G.-W. Moon are with the Korea Advanced Institute of Science and Technology, Daejeon 305-701, South Korea (e-mail: hanjk715@kaist.ac.kr; gwmoon@kaist.ac.kr).

J.-W. Kim is with the Virginia Tech Future Energy Electronics Center, Blacksburg, VA 24061 USA (e-mail: jwkim@vt.edu).

Color versions of one or more of the figures in this letter are available online at http://ieeexplore.ieee.org.

Digital Object Identifier 10.1109/TPEL.2017.2675283

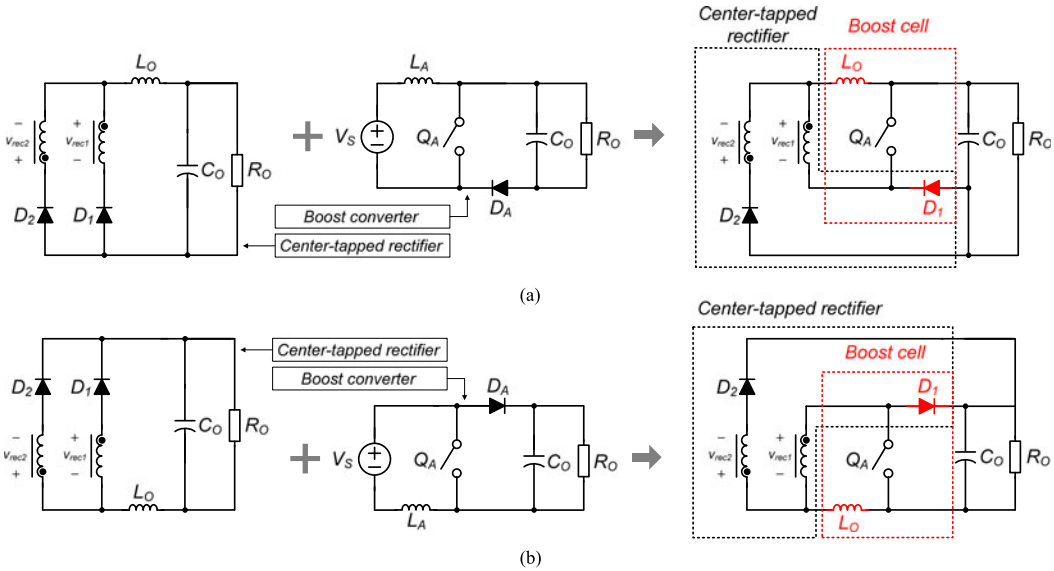

Fig. 2. Derivation of the proposed rectifier. (a) Type-1 rectifier and (b) type-2 rectifier.

with the conventional AHB converter. When AC loss occurs, the Q_A is turned on, and the output voltage is regulated using the additional voltage gain of the cascaded boost converter. Thus, because the cascaded boost converter compensates for the hold-up time, the AHB converter can be designed regardless of the wide input voltage range which solves the aforementioned problems such as the small duty-ratio, the large DC offset current in the transformer and the small transformer turns-ratio. However, regrettably, the boost diode D_A located in the main current path causes an additional conduction loss even though the boost switch Q_A is not turned ON. Therefore, a new method is essential to solve the aforementioned problems without any additional conduction loss.

In this letter, a new boost-integrated AHB converter is proposed. Compared to the conventional boost-cascaded AHB converter, a boost-integrated rectifier of the proposed converter does not cause any additional conduction loss in the nominal state because the main current does not flow through the additional components. Therefore, the proposed rectifier enabling the AHB converter can be designed optimally in the nominal state regardless of the hold-up time.

This letter is an extended version of "Efficiency Optimized Asymmetric Half-Bridge Converter With Hold-Up Time Compensation [1]" in *Proc. IEEE Power Electron Conf.*, May 2016. This version focuses on a secondary rectifier especially about derivation and intuitive understanding.

II. Derivation of the Proposed Converter

Fig. 2 shows the derivation of the boost-integrated rectifier for proposed converter. As shown in Fig. 2(a), the proposed rectifier merges the center-tapped rectifier and boost converter. To integrate the boost converter in rectifier, an additional switch Q_A is added, while L_A and D_A are merged with L_O and D_1. The current direction of Q_A should be unidirectional and it can be realized with a switch and a diode.

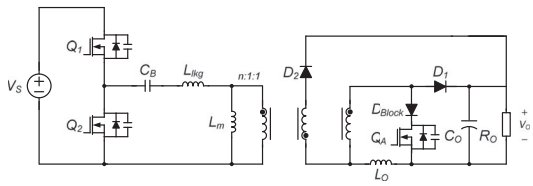

Fig. 3. Proposed converter.

Compared with the boost-cascaded rectifier shown in Fig. 1(b), the proposed rectifier does not cause a conduction loss at the boost diode in the nominal state since it merges the boost diode D_A and rectifier diode D_1. As a result, the proposed rectifier operates exactly the same as the conventional AHB converter in the nominal state since the integrated boost converter is used only during the hold-up time.

Fig. 2(b) shows another structure of the proposed rectifier. Compared with a type-1 rectifier shown in Fig. 2(a), type-2 rectifier has advantage that it does not need a floating gate driver. In case of using synchronous rectifiers (SRs), the type-1 rectifier can be better choice since the type-2 rectifier needs two floating gate drivers for SRs.

III. Operational Principle

The proposed converter has different operational principle during the nominal and hold-up state, since it utilizes the integrated boost converter during the hold-up state only. The operational principle of the proposed converter is analyzed in the nominal state and hold-up state. The proposed converter with type-2 rectifier shown in Fig. 3 is discussed in this letter.

A. Operational Principle in the Nominal State

In the nominal state, since the additional switch is turned off, the proposed converter has the same circuit structure with

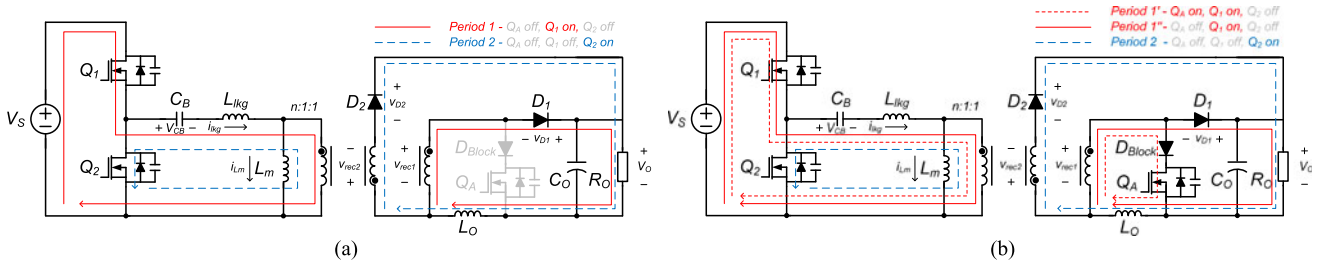

Fig. 4. Operational principle of the proposed converter. (a) Nominal state and (b) hold-up state.

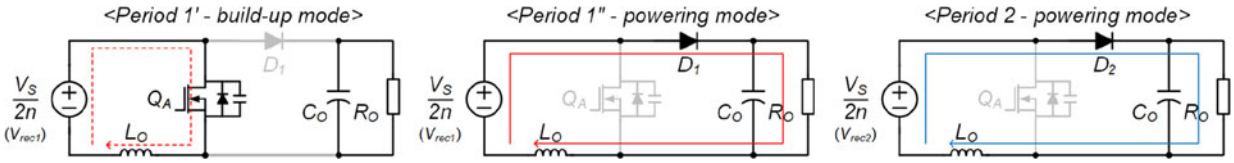

Fig. 5. Equivalent circuit of the proposed converter during the hold-up time.

the conventional AHB converter as shown in Fig. 4(a). The operational principle is also the same with the conventional AHB converter except that the proposed converter is designed to use a duty-ratio of the Q_1 as 0.5 in the nominal state. During the period 1, where the Q_1 is turned on and the Q_2 is turned off, main current flows through the red line path shown in Fig. 4(a). And during the period 2, the main current flows through the blue dashed-line path. Because the integrated boost cell is not conducted during the whole switching period, the additional conduction loss does not occur while it enables the proposed converter to have the maximum duty-ratio of the Q_1.

B. Operational Principle in the Hold-Up State

In the hold-up state the hold-up time, the boost switch Q_A is turned on to obtain the additional voltage gain by boost converter operation. As shown in Fig. 4(b), the Q_A and Q_1 are turned on during the period $1'$ and the integrated boost converter utilizes the rectifier voltage $V_{\rm rec}$ as an input voltage source. And during the period $1'$, the main current flows through the red short-dashed-line which builds-up an energy to the output inductor. When the Q_A is turned off, the period $1''$ starts, and the energy built-up during the period $1'$ is transferred to the output through the red-line, same with the boost converter. And during the period 2, the energy built-up during the period $1'$ is still transferred to the output while the current path is just changed to blue dashed-line from red-line.

The boost converter operation can be more intuitively understood with an equivalent circuit of the proposed converter. As shown in Fig. 5, the proposed converter operates the same with the boost converter, which utilizes the rectifier voltage as an input voltage source. The rectifier voltages $v_{\rm rec1}$ and $v_{\rm rec2}$ are obtained as follows:

$$v_{\rm rec1} = (V_S - V_{CB})/n = (1 - D_{Q1})V_S/n = V_S/2n \quad (1)$$

$$v_{\rm rec2} = V_{CB}/n = D_{Q1}V_S/n = V_S/2n \quad (2)$$

where the D_{Q1} and D_{Q2} are duty-ratio of the switch Q_1 and Q_2, $V_{CB} = D_{Q1}V_S$ by voltage–second equation to the transformer, and $D_{Q1} = D_{Q2} = 0.5$. In terms of the boost converter operation, the period $1'$ is the build-up mode and the period $1'''$ and period 2 are the powering mode, while the boost diode is just changed D_2 from D_1. As a result, the proposed converter operates like a two-stage structure consists of the AHB converter and boost converter, and the voltage gain is also obtained as a multiplication of voltage gains of two converters. However, since the boost converter utilizes the $V_{\rm rec1}$ during the powering mode, Q_A must be turned on when the $V_{\rm rec1}$ is positive and this makes the Q_A be turned on within the D_{Q1}.

IV. Characteristics of the Proposed Converter

A. Voltage Gain Comparison

Fig. 6 shows a normalized voltage gain graph of the conventional AHB converter and the proposed converter based on the voltage gain formula in Table I. As shown in Fig. 6(a), the conventional AHB converter is designed to have $D_{Q1} = 0.5$ during the hold-up state, where the input voltage is the lowest since the voltage gain is maximum at $D_{Q1} = 0.5$. As a result, unavoidably, the large DC offset current in the transformer occurs in the nominal state since it uses small duty-ratio when input voltage is high. Also, because the transformer turns-ratio is determined with the low-input voltage, it is designed to have a small value resulting in a large primary RMS current and large voltage stresses on a secondary rectifier.

On the other hand, as shown in Fig. 6(b), the proposed converter utilizes the additional voltage gain of the integrated boost converter to compensate low-input voltage during the hold-up time. Therefore, Q_1 operates with 0.5 duty-ratio in the nominal state regardless of the hold-up time and the DC offset current in the transformer does not occur. Also, the transformer turns-ratio can be higher, since it is designed at the nominal state where the input voltage is high. So, the primary RMS current and volt-

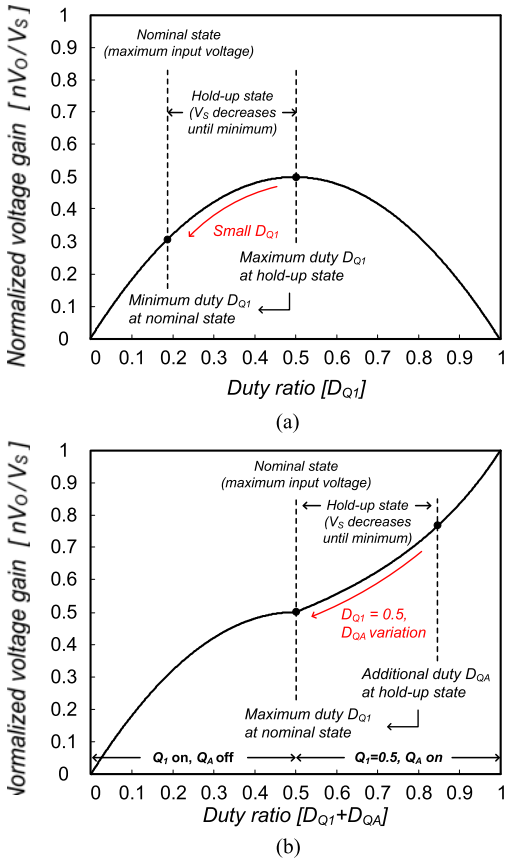

Fig. 6. Normalized voltage gain graph. (a) Conventional AHB converter and (b) proposed converter.

TABLE I
CHARACTERISTICS OF THE CONVERTERS

	Conventional AHB converter	Proposed converter
Voltage gain	$\frac{V_O}{V_S} = \frac{2D_{Q1}(1-D_{Q1})}{n}$	$\frac{V_O}{V_S} = \frac{2D_{Q1}(1-D_{Q1})}{n} \cdot \frac{1}{1-D_{QA}}$
Duty-ratio D_{Q1} in the nominal state	*Minimum duty*	*Maximum duty*
DC offset current in the transformer	*Large*	*Zero*
Transformer turns-ratio n	*Small*	*Large*

age stresses on the secondary rectifier are also reduced. These characteristics are summarized in Table I.

From these advantages, the proposed converter can reduce the size of the transformer and primary conduction loss. Additionally, by using a diode with a low voltage rating, the forward voltage drop and reverse recovery current in the rectifier diodes can be decreased. As a result, the proposed converter achieves a high efficiency in the nominal state, where the efficiency is the most important.

B. Comparisons With a Cascaded Boost Converter

As mentioned before, the boost switch Q_A must be turned on synchronously with the half-bridge switch Q_1 since the integrated boost converter utilizes the v_{rec1} as an input source. And it makes the duty-ratio of D_{QA} be limited to 0.5 and the maximum boost gain is double. But in the case of the cascaded boost converter, since it can have larger duty-ratio than 0.5, it has wide input voltage range resulting in large hold-up time or a small link capacitor. However, although the cascaded boost converter has large hold-up time, the proposed converter can achieve high efficiency because it eliminated the additional conduction loss at diode in nominal state. Therefore, the proposed converter is appropriate topology for high-efficiency AHB converter.

C. Design Considerations of the Integrated Boost Converter

In the proposed converter, a design of the secondary rectifier is important because it not only decides the hold-up time but also affects an output inductor and capacitor by boost converter operation.

The hold-up time is related with the link capacitor and input voltage range. Since the link capacitor can be reduced when the input voltage range is large, the proposed converter should be designed to have large input voltage range. Suppose that the input voltage range is $V_S \sim \frac{1}{2}V_S$ with maximum boost gain, the hold-up time is obtained as follows:

$$t_{\mathrm{hold}} = \eta\left(\frac{1}{2}C_{\mathrm{Link}}{V_{S,\mathrm{nom}}}^2 - \frac{1}{2}C_{\mathrm{Link}}{V_{S,\mathrm{min}}}^2\right)/P_O = \eta\left(\frac{3}{8}C_{\mathrm{Link}}{V_{S,\mathrm{nom}}}^2\right)/P_O \quad (3)$$

where the t_{hold} is a hold-up time, η is a converter efficiency, C_{link} is a link capacitor, $V_{S,\mathrm{nom}}$ is a nominal voltage of the link capacitor, $V_{S,\mathrm{min}}$ is a minimum voltage of the link capacitor, and P_O is an output power.

And since the proposed converter integrates the boost converter in the secondary rectifier, an output inductor and capacitor have characteristics of the boost converter resulting in large inductor ripple and discrete output current during the hold-up time. The inductor ripple and current stress of the output capacitor are obtained as follows:

$$\Delta I_{LO,p-p} = \frac{v_{\mathrm{rec1}}D_{QA}}{L_O f_s} \quad (4)$$

$$I_{\mathrm{CO,RMS}} = \frac{1}{T_S}\sqrt{\int_0^{D_{QA}T_S}(-I_O)^2dt + \int_{D_{QA}T_S}^{T_S}\left(\frac{D_{QA}}{1-D_{QA}}I_O\right)^2 dt} \quad (5)$$

where the $\Delta I_{LO,p-p}$ is an inductor ripple, f_s is a frequency of Q_1, $I_{\mathrm{CO,RMS}}$ is the current stress of the output capacitor, and I_O is a output current. Since a frequency of Q_A is the same with Q_1 and the maximum duty-ratio is 0.5, the largest voltage ripples are obtained as $\frac{v_{\mathrm{rec1}}}{2L_O f_s}$, I_O when $D_{QA} = 0.5$.

V. EXPERIMENTAL RESULTS

The effectiveness and feasibility of the proposed converter were verified with experimental results. Design examples for experiment are listed in Table II. Fig. 7 shows the waveforms of the conventional AHB converter and the proposed converter

TABLE II
DESIGN EXAMPLES

	Conventional AHB	DCS HB	Boost-cascaded AHB	Proposed
Input voltage range	250–400 V	250–400 V	100–400 V	250–400 V
Primary switches (Q_1, Q_2)	IPP60R600(600 V, 600 mΩ)			
Duty-ratio in the nominal state	0.19	0.3	0.38	0.38
DC offset current in the transformer ($I_{Lm\,\mathrm{offset}}$)	1.02	0	0.19	0.19
Transformer core	PQ2620 (5490 mm^3)	PQ2020 (2790 mm^3)	PQ2020 (2790 mm^3)	PQ2020 (2790 mm^3)
Turns-ratio (n)	40:20:20	62:26:26	81:20:20	81:20:20
Voltage stress of rectifier diode1 (V_{D1})	76 V	168 V	75 V	75 V
Voltage stress of rectifier diode2 (V_{D2})	324 V	168 V	122 V	122 V
Rectifier diode (D_1)	MBR20150CTP (150 V, 0.75 V_F)	MBR40250G (250 V, 0.8 V_F)	MBR20150CTP (150 V, 0.75 V_F)	MBR20150CTP (150 V, 0.75 V_F)
Rectifier diode (D_2)	IDT12S60C (600 V, 1.2 V_F)	MBR40250G (250 V, 0.8 V_F)	MBR40250G (250 V, 0.8 V_F)	MBR40250G (250 V, 0.8 V_F)
Additional switch (Q_A)	–	IPP60R600 (600 V, 600 mΩ)	IPP80CN10N (100 V, 80 mΩ)	IPP80CN10N (100 V, 80 mΩ)
Additional diode (D_A)	–	MBR4 0250 (250 V, 0.8 V_F)	MBR20100CTG (100 V, 0.8 V_F)	MBR20100CTG (100 V, 0.8 V_F)
Link capacitor (C_{Link})	164 μF	164 μF	164 μF	164 μF
Hold-up time	48 ms	48 ms	72 ms	48 ms

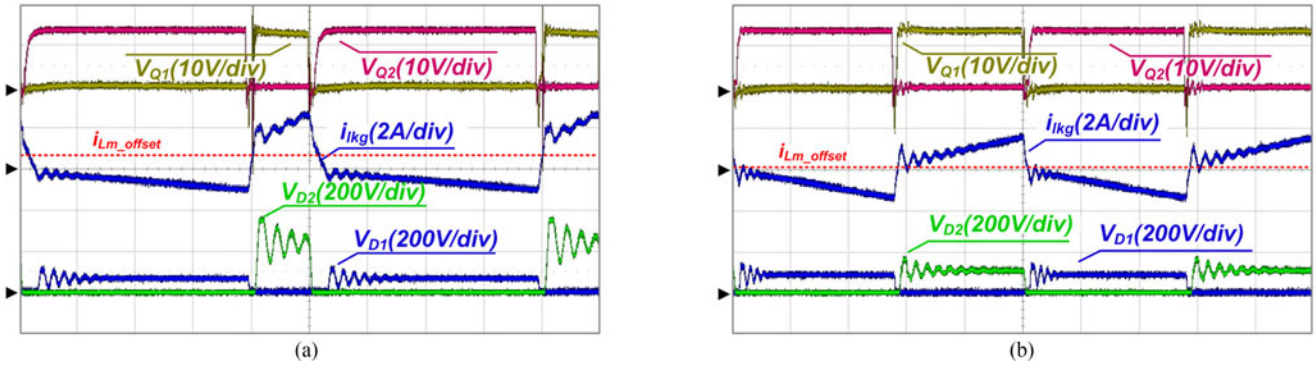

Fig. 7. Waveforms of the prototype converters with 400-V input, 3.3 A/45 V output. (a) Conventional AHB converter and (b) proposed converter.

in the nominal state with a full load condition (400-V input, 45 V/3.3 A output). As mentioned before, the conventional AHB converter has a large DC offset current I_{Lm_offset} in the transformer due to the small duty-ratio of Q_1 as shown in Fig. 6(a). Additionally, because of the small transformer turns-ratio, it has the large primary RMS current and large voltage stresses on the rectifier diodes. On the other hand, as shown in Fig. 7(b), the proposed converter has a small I_{Lm_offset} since the proposed converter operates with the large duty-ratio. Also, the primary RMS current and voltage stresses on the rectifier diodes are considerably reduced compared with the conventional AHB converter. Although the duty-ratio of the Q_1 is 0.5 in ideal case, it is designed to be slightly smaller than 0.5 considering 120-Hz ripple of the input voltage in actual case.

Fig. 8 shows the waveforms of the transient operation during the hold-up time. When AC loss occurs, the boost switch Q_A is turned on to regulate the output voltage constantly. As shown in figure, the output voltage is tightly regulated during the hold-up time while the input voltage decreases continuously.

Fig. 9 shows the measured efficiencies of the prototype converters in the nominal state. As mentioned before, the proposed converter achieved the high efficiency in the overall load condition compared to the conventional AHB converter because it has a small DC offset current in the transformer, a small primary RMS current, and small voltage stresses on the rectifier diodes. The boost-cascaded AHB converter also achieved the high efficiency, but the additional conduction loss at the boost diode D_A degraded the overall efficiency. Also, the DCS HB converter has low efficiency compared with these converters

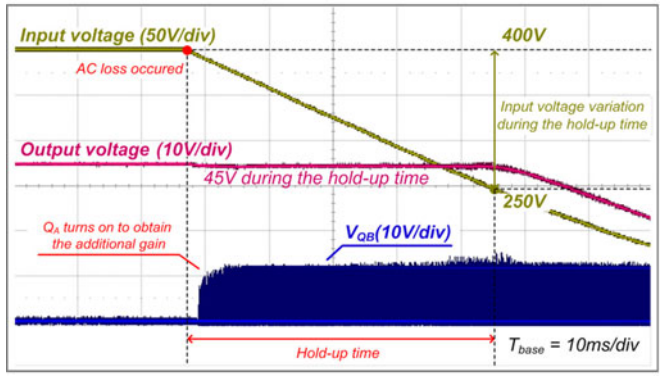

Fig. 8. Transient operation during the hold-up time.

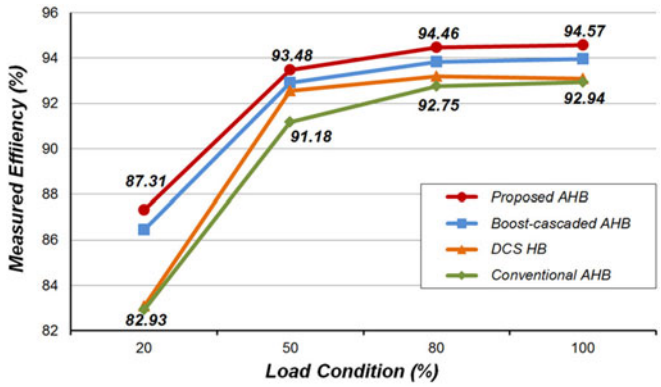

Fig. 9. Measured efficiency.

due to small transformer turns-ratio and additional conduction losses at switch Q_A and diode D_A.

VI. Conclusion

In this letter, a boost-integrated AHB converter is proposed. The proposed converter integrates a boost converter in the rectifier in a new manner. Because the proposed converter can obtain an additional voltage gain during a hold-up time, it can be designed optimally in the nominal state regardless of the hold-up time requirement. Furthermore, since the proposed converter does not cause an additional loss in the nominal state, it can achieve the optimized efficiency.

References

[1] J. K. Han, J. W. Kim, and G. W. Moon, "Efficiency optimized asymmetric half-bridge converter with hold-up time compensation," in *Proc. IEEE Power Electron. Conf.*, May 2016, pp. 2254–2261.

[2] H. Wu, T. Mu, X. Gao, and Y. Xing, "A secondary-side phase-shift-controlled LLC resonant converter with reduced conduction loss at normal operation for hold-up time compensation application," *IEEE Trans. Power Electron.*, vol. 30, no. 10, pp. 5352–5357, Oct. 2015.

[3] Y. S. Lai, Z. J. Su, and W. S. Chen, "New hybrid control technique to improve light load efficiency while meeting the hold-up time requirement for two-stage server power," *IEEE Trans. Power Electron.*, vol. 29, no. 9, pp. 4763–4775, Sep. 2014.

[4] D. K. Kim, S. Moon, C. O. Yeon, and G. W. Moon, "High-efficiency LLC resonant converter with high voltage gain using an auxiliary LC resonant circuit," *IEEE Trans. Power Electron.*, vol. 31, no. 10, pp. 6901–6909, Oct. 2016.

[5] J. B. Lee, J. K. Kim, J. H. Kim, J. I. Baek, and G. W. Moon, "A high-efficiency PFM half-bridge converter utilizing a half-bridge LLC converter under light load conditions," *IEEE Trans. Power Electron.*, vol. 30, no. 9, pp. 4931–4942, Sep. 2015.

[6] M. Arias, M. F. Diaz, D. G. Lamar, F. F. Linera, and J. Sebastian, "Small-signal and large-signal analysis of the two-transformer asymmetrical half-bridge converter operating in continuous conduction mode," *IEEE Trans. Power Electron.*, vol. 29, no. 7, pp. 3547–3562, Jul. 2014.

[7] W. Li, Y. He, Y. Sun, F. Wang, and L. Ma, "Series asymmetrical half-bridge converters with voltage autobalance for high input-voltage applications," *IEEE Trans. Power Electron.*, vol. 28, no. 8, pp. 3665–3674, Aug. 2013.

[8] M. Arias *et al.*, "Design of a soft-switching asymmetrical half-bridge converter as second stage of an LED driver for street lighting application," *IEEE Trans. Power Electron.*, vol. 27, no. 3, pp. 1608–1621, Mar. 2012.

[9] H. S. Lee, H. J. Choe, S. H. Ham, and B. Kang, "High-efficiency asymmetric forward-flyback converter for wide output power range," *IEEE Trans. Power Electron.*, vol. 32, no. 1, pp. 433–440, Jan. 2017.

[10] J. B. Lee, K. B. Park, J. K. Kim, H. S. Youn, and G. W. Moon, "A new center-tapped half-bridge zeta converter with small transformer dc-offset current and low voltage stress," *IEEE Trans. Power Electron.*, vol. 30, no. 12, pp. 6593–6603, Dec. 2015.

[11] I. O. Lee and G. W. Moon, "A new asymmetrical half-bridge converter with zero DC-offset current in transformer," *IEEE Trans. Power Electron.*, vol. 28, no. 5, pp. 2297–2306, May 2013.

[12] M. Hong, J. A. Qahouq, S. Luo, and I. Batarseh, "Zero-voltage-switching half-bridge DC-DC converter with modified PWM control method," *IEEE Trans. Power Electron.*, vol. 19, no. 4, pp. 947–958, Jul. 2004.

[13] C. Yao, X. Ruan, X. Wang, and C. K. Tse, "Isolated buck-boost DC/DC converters suitable for wide input-voltage range," *IEEE Trans. Power Electron.*, vol. 26, no. 9, pp. 2599–2613, Sep. 2011.